Journal of Power Sources 196 (2011) 3803–3809

Contents lists available at ScienceDirect

Journal of Power Sources

journal homepage: www.elsevier.com/locate/jpowsour

Effect of cation contamination and hydrated pressure loading on the mechanical properties of proton exchange membranes

Ruiliang Jia[a], Binghong Han[a], Kemal Levi[a], Takuya Hasegawa[b], Jiping Ye[c], Reinhold H. Dauskardt[a,*]

[a] Department of Materials Science and Engineering, Stanford University, Stanford, CA 94305, USA
[b] Nissan Research Center, Nissan Motor Co., Ltd., 1 Natsushima-cho, Yokosuka 237-8523, Japan
[c] Research Department, Nissan ARC Ltd., 1 Natsushima-cho, Yokosuka 237-0061, Japan

ARTICLE INFO

Article history:
Received 25 October 2010
Received in revised form
15 December 2010
Accepted 16 December 2010
Available online 24 December 2010

Keywords:
Perfluorosulfonic acid polymer
Proton exchange membrane
Nafion®
Bulge test
Tearing
Cation exchange

ABSTRACT

Perfluorosulfonic acid (PFSA) polymer membranes are widely used as electrolyte thin films to transport protons in proton exchange membrane (PEM) fuel cells. The mechanical degradation of the membrane represents a common failure mode that limits the operational life of the fuel cells. In the present work, effect of contamination related to cation exchange on the mechanical reliability of PEMs was investigated. We applied the bulge test technique to assess the mechanical properties of Nafion® PFSA membranes simulating pressure loading on hydrated PEMs in fuel cells. The corresponding elastic moduli of Nafion® before and after cation exchange were analyzed and compared with the results measured by uniaxial tension experiments at selected humidity conditions, showing increasing stiffness with the increase of cation radius. We also used the out-of-plane tearing test method to characterize the fracture behaviors of PEMs. The effects of cation exchange and water absorption on mechanical and fracture properties of PEMs at different temperatures are discussed in terms of cation and water interactions with the molecular structure of PFSA polymers.

1. Introduction

Perfluorosulfonic acid (PFSA) polymer membranes are widely used as electrolyte thin films to transport protons in proton exchange membrane (PEM) fuel cells [1,2]. It has been observed that mechanical degradation of PEMs is a common failure mode, which occurs more easily in stress concentration areas, and near the boundary region between reaction and non reaction zones that exist in the membranes [2–4]. In addition, contamination due to impure reactant gases and corrosion of tubing or fitting materials that results in cation exchange in the PEM tends to deteriorate fuel cell performance [5], and may be implicated in the acceleration of mechanical degradation.

Accordingly, in this research we investigated the effect of foreign cation contamination on the mechanical properties of PEMs. The bulge testing method using water as a pressure medium was applied to simulate pressurized loading on hydrated PEMs in fuel cells. This method has been previously used with a gas pressure medium to characterize PEMs' strength and resistance to gas leakage [6–8]. We characterized the biaxial stress–strain behavior of the membranes under fully hydrated conditions. Foreign cation contamination was assessed by comparing the resulting elastic deformation behavior of PEMs after exchange with selected cations (Fe^{3+}, Mg^{2+}, Cu^{2+}, Li^{+}, Na^{+} and K^{+}) with that of as-received membranes (Naifon-H^{+}), showing increased stiffness with the increase of cation radius. The bulge technique was also used to measure the pressure dependant water penetration and onset of leaking through the membranes.

We also used the out-of-plane tearing test method to characterize the fracture behavior of the PEMs. Both cation exchange and water absorption had deleterious effects on the fracture resistance of the membranes, which was rationalized in terms of the interaction of the cation and water with the molecular structure of PFSA polymers.

2. Experimental

2.1. Materials

Nafion® NRE 211 membranes from Du Pont®, with a nominal thickness of 0.025 mm, were used as a representative of PEM in the experiments. The as-received membranes are in acid form (Nafion-H^{+}). Salt forms of the Nafion® membrane were prepared

Abbreviations: PFSA, perfluorosulfonic acid; PEM, proton exchange membrane; DIW, distilled water.

* Corresponding author at: Department of Materials Science and Engineering, 496 Lomita Mall, Durand Bldg., Room 121, Stanford University, Stanford, CA 94305-2205, USA. Tel.: +1 650 725 0679; fax: +1 650 725 4034.
E-mail address: rhd@stanford.edu (R.H. Dauskardt).

0378-7753/$ – see front matter © 2011 Elsevier B.V. All rights reserved.
doi:10.1016/j.jpowsour.2010.12.066

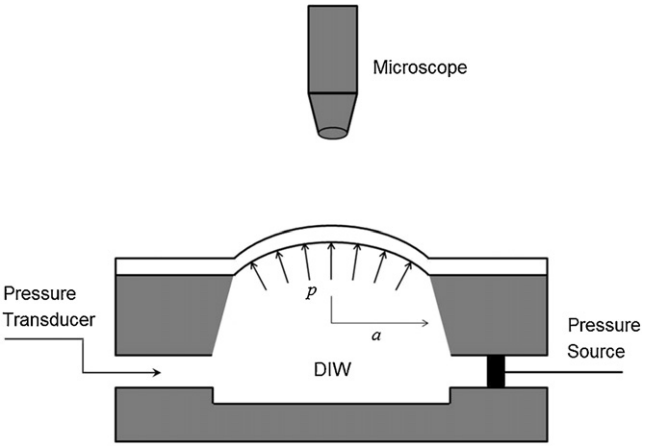

Fig. 1. Schematic diagram of the bulge test apparatus.

in the similar procedures used by Kawano et al. [9]: the as received Nafion® samples were soaked in 1 M aqueous solutions of respective salts (LiCl, NaCl KCl, $MgCl_2$, and $CuSO_4$) and 0.5 M $Fe_2(SO_4)_3$ at 23 °C for 24 h, then repeatedly rinsed in distilled water (DIW) to remove the excess electrolyte, and wiped with filter paper. Finally, the treated membranes were dried at 30 °C for 24 h before use. The membrane thickness of each specimen was measured with a digital micrometer (Digimatic Micrometer, Mitutoyo Corporation, Japan) prior to experiments.

2.2. Bulge test

Bulge testing was conducted using the experimental arrangement shown in Fig. 1. The heart of the bulge test system is a plexiglass unit encasing a drilled cavity with two channels, which were filled with DIW as the medium to better simulate the hydrated pressure loading on PEMs in fuel cells. A syringe plunger (1705 RN, Hamilton Co., Reno, Nevada) controlled by a high precision DC motor was used to apply the pressure inside the system, which were simultaneously measured by a pressure transducer (Model 210, Precision Measurement Co., Ann Arbor, MI). All components of the apparatus were threaded and sealed using a silicone-based gasket compound to prevent DIW from leaking.

Nafion® specimens (15 mm × 15 mm) were first clamped onto the orifice of the cavity, touching the DIW medium with great care to avoid air hidden inside the system and to minimize residual stress in the membranes, and after exposure to DIW for 10 min the membranes were pressurized with the medium. Specimens were observed to form a balloon-like shape as the syringe plunger was pushed at a displacement rate of 100 μm s^{-1}, and the resulting medium flow rate was 0.089 μL s^{-1}. The bulge test system was positioned inside an environment chamber (Associated Environmental System, Inc., Ayer, MA) and the experiments were carried out at a constant relative humidity (25% RH) and at temperatures of 23 °C and 80 °C which was used to simulate the typical operating temperature of PEMFCs. During the experiments, an optical microscope was used to measure the bulge height, and another was positioned vertically above the bulge system to monitor the water penetration on the surface of the bulged membrane, as shown in Fig. 1.

To determine the biaxial stress and strain in the PEM, the pressurized membrane was modeled as a section of a thin-walled spherical pressure vessel having uniform equal biaxial stress and curvature. Then, the equal biaxial stress, σ, in the membranes was given by:

$$\sigma = \frac{pR}{2t} \tag{1}$$

where p is the applied pressure, R is the radius of the sphere and t is thickness of the tissue. Using the Pythagorean Theorem, the radius of pressure orifice, a, and bulge height, h, was related to R:

$$R = \frac{h}{2} + \frac{a^2}{2h} \tag{2}$$

The bulge height h of the PEM specimens was measured with optical microscopy from the side view by focusing on the highest center of bulged specimens.

The thickness of the bulged membrane was calculated assuming constant volume deformation with the equation:

$$t = \frac{t_0}{\lambda^2} \tag{3}$$

where t_0 is the initial, strain-free thickness of the PEM measured before clamping on the test system, and λ is the biaxial stretch given by:

$$\lambda = \frac{L}{2a} \tag{4}$$

where L is the length of the arc of the bulge. The biaxial true strain, ε, was obtained from the biaxial stretch using:

$$\varepsilon = \ln(\lambda) \tag{5}$$

The biaxial modulus B of the membrane was determined from the initial slope of stress–strain curves before the onset of non-linear yield loading. Assuming isotropic material property for the PFSA polymer, the Young's modulus was found using:

$$E = B(1 - \nu) \tag{6}$$

where ν is Poisson's ratio of PFSA polymers, and is assumed to be a typical value of polymer materials $\nu = 0.4$ for all membranes in this study.

2.3. Uniaxial tension test

The elastic moduli of the membranes were also determined using uniaxial tension tests, which were conducted with a mechanical test system (MTS 810, MTS Systems Corporation, Eden Prairie, MN) with an environment control chamber (AVS Applied Test Systems, Inc., Butler, PA). Membranes were measured at combinations of two different temperatures (23 °C and 80 °C) and two different relative humilities (25% and 100%). At every temperature and humidity combination, three specimens (10 mm × 80 mm) of each type of membranes were first treated in the relevant environment for 30 min and then loaded in tension at a constant crosshead speed of 100 μm s^{-1}. The elastic moduli were determined from the initial range of the stress–strain curves, and the average values for each type of specimens were reported.

2.4. Out-of-plane tearing test

The out-of-plane tearing test (trouser test) specimen is shown in Fig. 2. The pre-crack was created with a surgery blade, making two legs with an identical width of 12.5 mm, and the ligament length was controlled ~22 mm. The tests were performed with a high precision mechanical test system (DTS Company, Menlo Park, CA) positioned inside an environment chamber (Associated Environmental System, Inc., Ayer, MA). The legs clamped in the testing machine were loaded in tension in opposite directions at a constant displacement rate of 100 μm s^{-1}, and out of plane fracture propagated in the ligament. The tearing fracture energy was calculated using [10,11]:

$$G_{\text{tear}} = \frac{2F}{t} \tag{7}$$

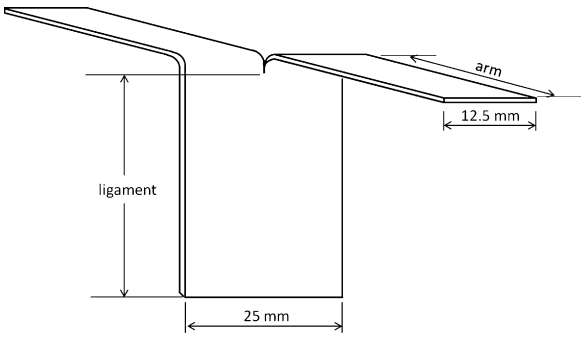

Fig. 2. Out-of-plane tearing test specimen.

where F is the average tearing force during fracture propagation and t is the thickness of the membrane. The out-of-plane tearing tests were conducted at 23 °C with 25% and 100% RH, respectively, to investigate the effect of water absorption, and also at 80 °C with 100% RH to simulate the operating environmental condition in PEMFCs. For each type of membrane, three specimens were tested.

3. Results and discussion

3.1. Bulge test on as received PEMs

The applied pressure on Nafion-H^+ membrane specimens at 23 °C with 25% RH is shown as a function of the pressurizing time in Fig. 3(a). The corresponding optical microscopy images of the bulge surface (top figures) and height (bottom figures) during the experiment are shown in Fig. 3(b). At a constant medium flow rate of 0.089 μL s^{-1}, the pressure within the system first increased linearly as a function of the pressurizing time, and then started yielding around 180 kPa (point a). At point b, DIW began penetrating through the membrane and tiny water drops appeared on the bulge surface. With increasing pressure, continuous leakage of water through the membrane occurred. After the maximum pressure point c, the pressure gradually decreased as water escaped through the membrane. Finally, the bulged membrane fractured at point e.

Based on the pressure data and the corresponding bulge height measured by the microscope II from the side view, the biaxial true stress and strain were calculated using Eqs. (1)–(5). As the stress vs. strain curve shows in Fig. 4, the biaxial stress initially increased linearly to a yielding point at ~0.02 strain, and then gradually increased with an increasing slope to a large strain. This represents the typical mechanical behavior of a hyper-elastic material.

3.2. Bulge test on PEMs after ion exchange

Fig. 5(a) illustrates the applied pressure as a function of the pressurizing time for the as received membrane and those exchanged with selected monovalent cations tested at 23 °C with 25% RH. It is observed that the initial slope of the p–t curves increased in the order of Li^+, Na^+ and K^+ cations. The comparison of the bulge height of the membranes with different ions exchanged vs. pressuring time in Fig. 5(b) shows little difference. As DIW continued penetrating the membrane and appeared on the bulge surface which prevented us from measuring the vertical deflection accurately,

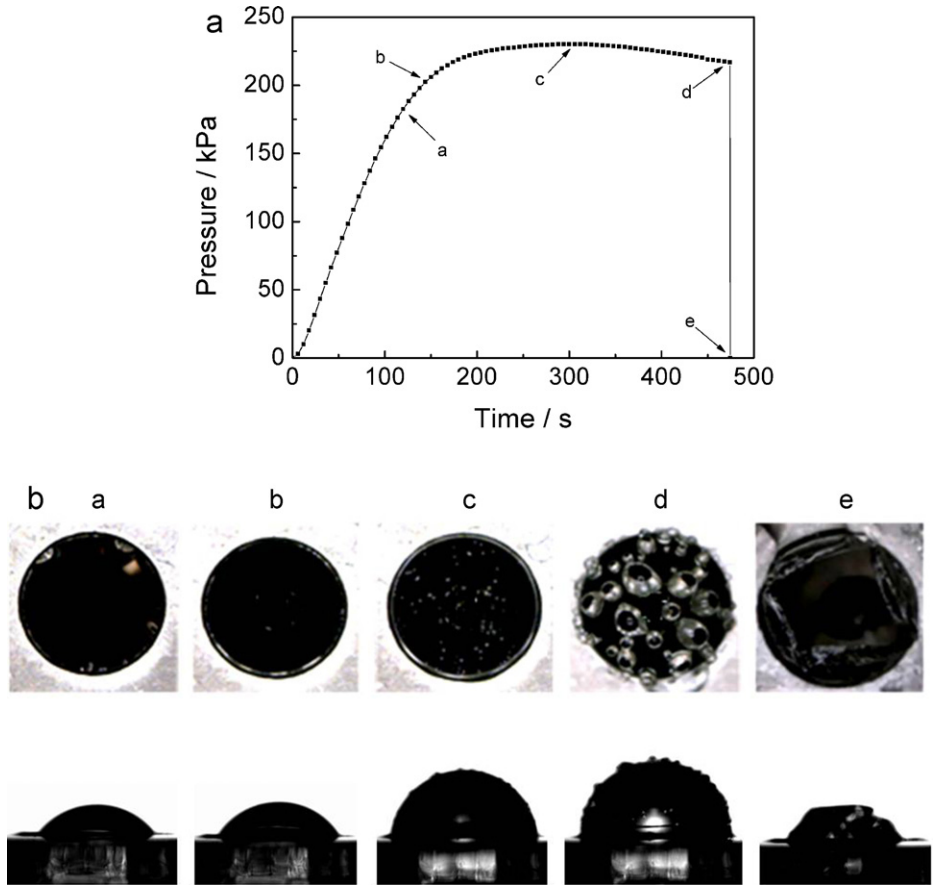

Fig. 3. (a) The applied pressure on the membrane as a function of the pressurizing time for as received Nafion®. (b) Optical microscopy images illustrating the bulge surface (top) and height (bottom) during the experiment.

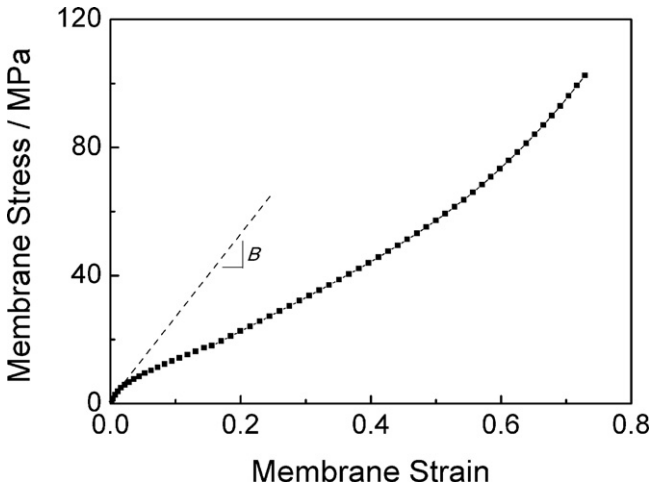

Fig. 4. Biaxial stress vs. strain of as received Nafion® membrane tested at 23 °C with 25% RH.

the bulge height measurement had to stop around 320 s in each experiment.

Using the data of applied pressure and bulge height, the biaxial stress and strain of ion exchanged membranes were calculated and compared with as received Nafion® in Fig. 6(a). All the stress–strain curves have the similar shape in the full strain range, but the stiffness of elastic deformation increased in the order of H^+, Li^+, Na^+ and K^+ ions, as illustrated in Fig. 6(b), which is similar to the result of uniaxial tensile test reported by Kawano et al. [9]. The biaxial moduli of membranes exchanged with divalent cations, Mg^{2+} and Cu^{2+}, and trivalent cations Fe^{3+} were also measured by the bulge tests. The average values of biaxial moduli B for each type of membrane tested at room temperature (23 °C) and the simulated operating temperature (80 °C) are reported in Table 1.

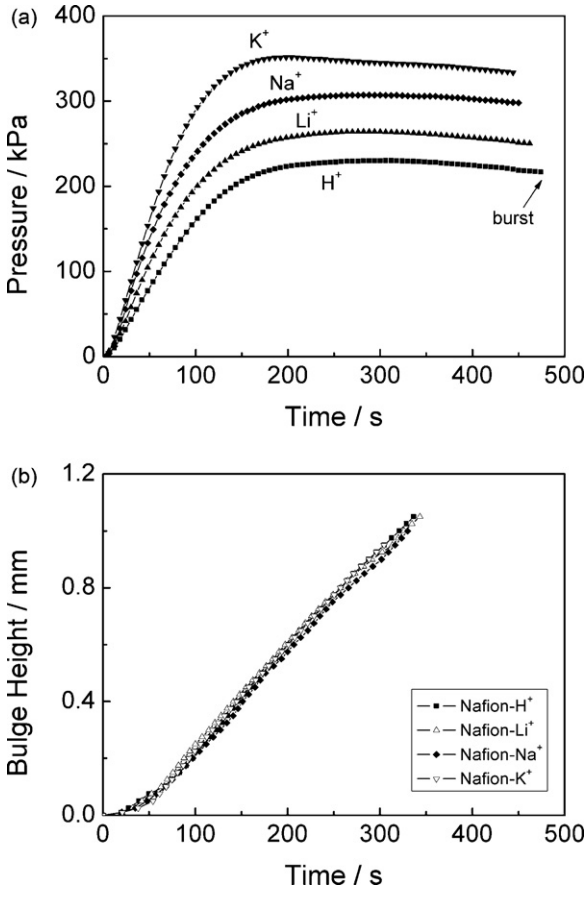

Fig. 5. (a) The applied pressure on the membranes as a function of the pressurizing time until burst and (b) bulge height as a function of pressurizing time for as received Nafion® membrane and cation exchanged membranes with monovalent cations (Li^+, Na^+ and K^+).

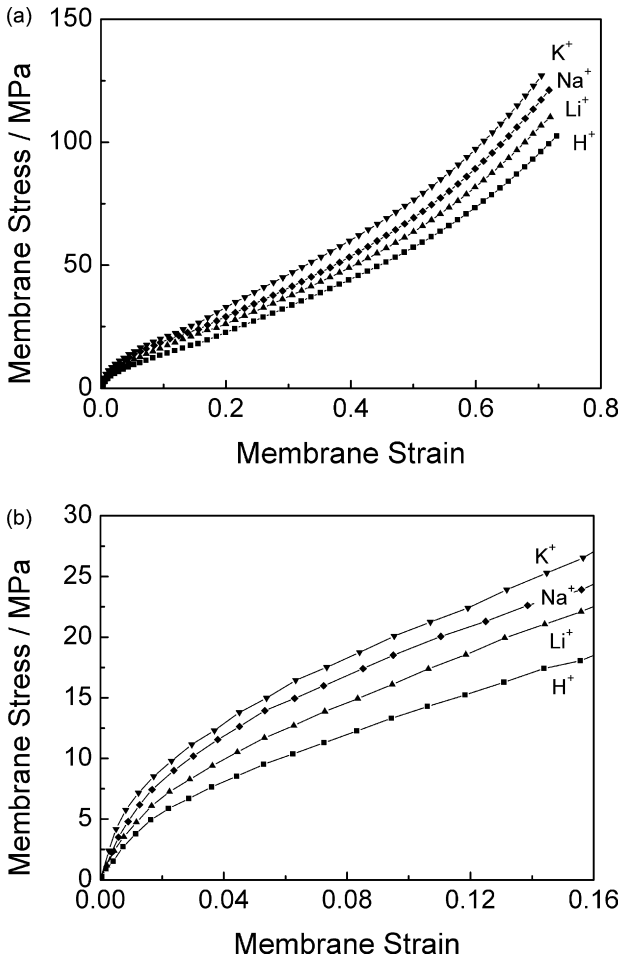

Fig. 6. Biaxial stress vs. strain of cation exchanged membranes with monovalent cations (Li^+, Na^+ and K^+) compared with as received Nafion® membrane (a) in full strain range and (b) in initial strain range 0–0.16.

3.3. Elastic modulus of PEMs

Based on the biaxial moduli B of membranes determined from the stress–strain curves above, we can calculate the corresponding Young's moduli E using Eq. (6), which are compared with the results measured by the uniaxial tension tests under four relevant environmental conditions in Table 1.

It is more instructive to compare the Young's moduli in terms of exchanged ionic radius under each temperature condition in Fig. 7(a) and (b). The as received membrane contains H_3O^+, whose radius was assumed to be the atomic radius of an oxygen atom [3]. From the comparisons in Fig. 7, we found that at both temperatures of 23 and 80 °C the Young's moduli E determined by the bulge test method were roughly equivalent to the results measured by the uniaxial tension experiments at 100% RH. This suggests that the pressure medium, DIW, diffused into the membranes under pressure loading and the membranes were hydrated during the bulge test.

In addition, it is noticeable that the Young's moduli of bulged membranes under hydration were much lower than their rela-

Table 1
Elastic moduli of Nafion® membranes before and after cation exchange determined by bulge test and uniaxial tension test.

Nafion® membranes	Biaxial modulus, B (MPa)		Young's modulus, E (MPa)					
	Bulge test $E = B \times (1 - \nu)$				Uniaixal tension test			
	23 °C	80 °C	23 °C	80 °C	23 °C		80 °C	
					25% RH	100% RH	25% RH	100% RH
Nafion-H^+	200.17	193.22	120.10	115.93	282.50	101.48	177.68	94.71
Nafion-Fe^{3+}	260.71	194.50	156.43	116.70	333.75	175.23	321.50	96.13
Nafion-Mg^{2+}	273.51	250.10	164.11	150.06	375.22	138.44	380.63	123.67
Nafion-Cu^{2+}	264.18	234.32	158.51	140.59	335.70	120.25	301.48	103.38
Nafion-Li^+	225.51	209.98	135.31	125.99	373.25	110.54	351	100.26
Nafion-Na^+	284.29	239.72	170.57	143.83	570	138.71	526	111.83
Nafion-K^+	317.89	275.70	190.73	165.42	890	231.54	757	127.95

tively dry counterparts (uniaxial tension test at 25% RH). This is due to plasticization of PFSA polymer by water absorption [12,13]. According to the cluster-network models of PFSA polymer [14–17], as water first diffuses into Nafion® membranes, the isolated clusters formed by sulfonic acid groups swells to be spherical water pools. With the increase of water absorption, the ionic interaction in the clusters is reduced. Besides, water existence might weaken the chain-to-chain bonding and further reduce the intermolecular forces. Both of these effects can cause the decrease in the membrane stiffness.

Based on the fitting lines for each case, we noticed that the Young's moduli of membranes increased linearly with increasing radius of cation exchanged. This should be implicated to the cations' affinity to the sulfonic acid groups in PFAS molecules [18–22]. Considering the cluster structures discussed above, the larger cations probably interact with more sulfonic acid groups and reduce the mobility of side chains, leading to the increasing stiffness of membranes. We also observed that the valence of cations exchanged has little effect on the elastic moduli of membranes, which were mainly governed by the ionic radius. A similar phenomenon for hydrated membranes measured by uniaxial tension tests in salt solutions was also reported by Kundu et al. [3]. They suggested that despite higher charge densities of multivalent cations the limited surface area of these cations prevents further physical cross-linking with other side chains in the PFSA molecules. In addition, the water content in the membranes exchanged with different cations could be another factor that influences the moduli of the membranes. It is known that the water fraction in the PFSA polymer membrane is related to the clusters size [22]. Even though multivalent cations can be assumed to bond with more sulfonic acid groups, their comparatively smaller size might induce higher water content if the volume of a cluster achieves its relatively constant upper limit. Thus the incorporation of smaller multivalent cations could probably enhance the weakening effect of water absorption on the stiffness of membrane.

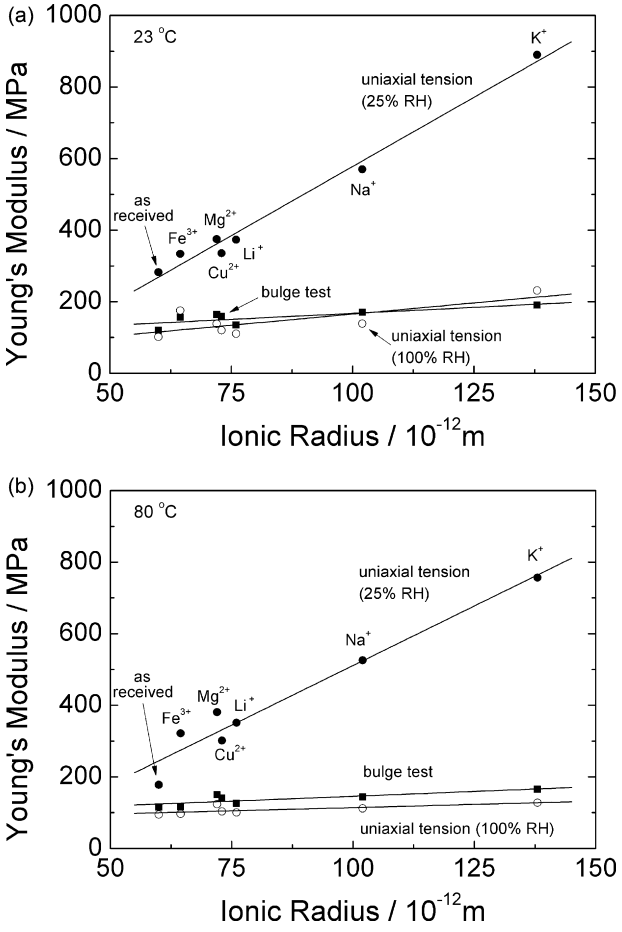

Fig. 7. Young's modulus of Nafion® membranes as a function of radius of selected cation exchanged tested at (a) 23 °C, and (b) 80 °C (●, uniaxial tension test at 25% RH; ■, bulge test; ○, uniaxial tension test at 100% RH).

By comparing the corresponding results in Fig. 7(a) and (b), we noticed that at a higher temperature of 80 °C the elastic moduli of all membranes under either dry or hydrated condition were slightly lower than their counterparts tested at 23 °C. This is in agreement with the results reported previously [23–26]. The increase of temperature tends to destroy the cluster structures and weaken the cross-linking of polymeric chains [9,23], which can increase the degree of elongation and reduce the stiffness of membranes.

3.4. Fracture behaviors of PEMs

The out-of-plane fracture propagated smoothly in the ligament of the tearing specimens with a relatively constant tearing force and a cracking path parallel to the arms. Fig. 8(a) shows the tearing force of as received Nafion® membrane compared with that of Nafion-Na, tested at 23 °C with 25% RH. There was an obvious decrease in the membrane tearing force after cation exchange. Moreover, we observed that the tearing force of as received membrane at 100% RH was much lower than that tested at 25% RH (Fig. 8(b)), indicating that water absorption can reduce the tearing resistance to a large extent. Based on the average values of the tearing force measured for each membrane (in the displacement range 10–40 mm), we calculated the corresponding tearing fracture energy, G_{tear}, using Eq. (7). G_{tear} values for membranes before and after cation exchange tested under relevant environment conditions are shown in Fig. 9.

We found a significant decrease in the tearing fracture energy for all membranes after cation exchange, compared with that of the as received membrane (Nafion-H^+) at 23 °C with 25% RH (clear bars). The harmful effect of cation contamination on the fracture

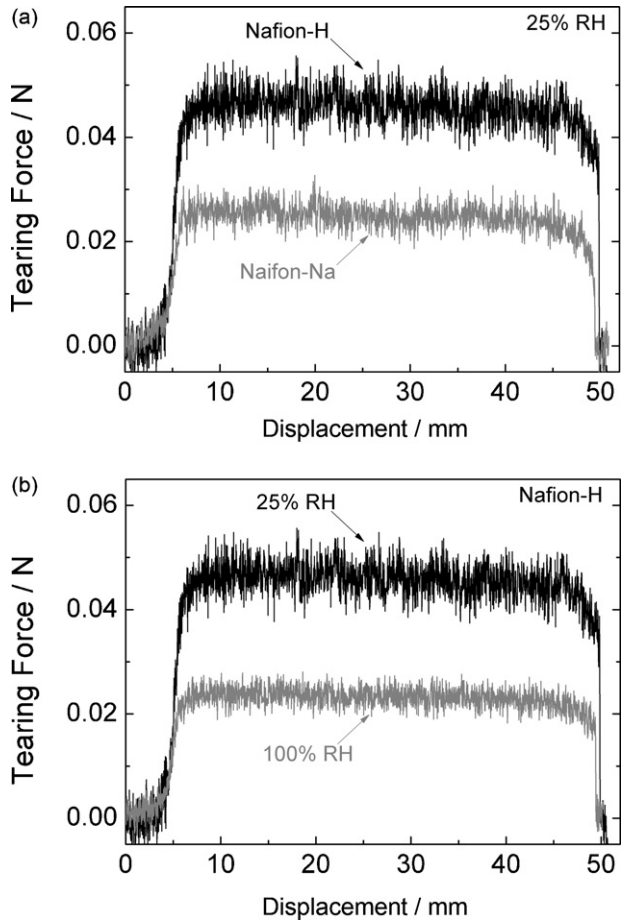

Fig. 8. Out-of-plane tearing forces of (a) Nafion-H^+ and Nafion-Na^+ tested at 23 °C with 25% RH and (b) Nafion-H^+ tested at 23 °C with different humidity conditions: 25% RH and 100% RH.

resistance may be related to the interaction of the cations with the PFSA molecular structure [3,9,18–22]. The foreign cations with larger radii presumably interact with more sulfonic acid groups. Moreover, the larger cations would absorb fewer water molecules in the clusters at a given humidity [22], which we expect will reduce the effect of water content on the ionic interactions. Both of these factors tend to decrease the mobility of the side chains, which probably lowers the flexibility of molecules around the clusters to form a glassy zone. Accordingly, fracture of the comparatively brittle glassy zones may occur with lower energy thus reducing the overall fracture resistance.

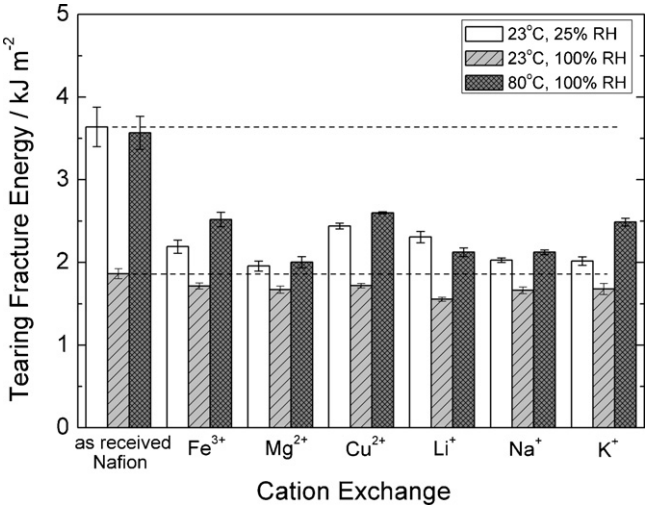

Fig. 9. Tearing fracture energy of as received Nafion® membranes and membranes after cation exchange under different environmental conditions.

The fracture energy G_{tear} of the as received membrane at 23 °C with 100% RH (clear bars) was significantly reduced compared to its dry counterpart measured at 25% RH (light grey bars), as shown in Fig. 9. The presence of excessive water in the membranes at 100% RH tends to not only weaken the ionic interaction in clusters, but also reduce the intermolecular forces of main chains in the PFSA polymers [12,27]. Meanwhile the density of membranes may decrease due to the swelling effect of water. All of these factors may lead to a decrease of fracture resistance. In addition, the G_{tear} values of cation exchanged membranes at 23 °C with 100% RH decreased dramatically and were slightly lower than the as received membrane. This indicates that the higher amounts of water absorbed in membranes could reduce the ionic interactions to more extent, but the foreign cations with larger radii might still interact with more sulfonic acid groups in the cluster structures than the original hydrogen ions, thereby forming a comparatively brittle glassy zone around the cluster. As a result, the stiffness of hydrated membranes after cation exchange increases (Fig. 7), and the fracture resistance was further reduced probably due to the formation of glassy zones in polymers (Fig. 9).

The tearing fracture energy G_{tear} values of the membranes tested at the simulated operating environment in PEMFCs (80 °C with 100% RH) are illustrated by the dark shaded bars in Fig. 9. It is noticeable that the fracture energies of all the membranes under the operating environmental condition were higher than their corresponding counterparts measured at 23 °C with 100% RH (light grey bars). According to previous reports that water content in Nafion® membranes decreases with increasing temperature at a given humidity [28,29], the harmful effect of water absorption on fracture resistance would be reduced at a higher temperature. However, we still observe significantly decreased fracture energies of membranes after cation exchange compared with that of as-received membranes, indicating that the comparatively brittle glassy zones discussed above may not be affected under the operating temperature condition and can still weaken the fracture resistance of membranes.

4. Conclusion

In this study, we investigated the effect of foreign cation contamination on mechanical properties of PEMs with various thin film characterization approaches. The bulge testing method was applied to assess the biaxial mechanical behavior of PEMs using water as a medium to better simulate hydrated pressurized loading on PEMs under operating environmental conditions in fuel cells. The elastic moduli of Nafion® membranes before and after cation exchange determined by bulge tests showed the same trend as those measured using uniaxial tension experiments under selected temperature and humidity conditions. The elastic moduli of PEMs increased with increasing radius of cation exchanged, but was reduced with the increase of water absorptions and temperature. In addition, we used the out-of-plane tearing test method to characterize the fracture properties of PEMs. The results showed that both cation exchange and water absorption had deleterious effects on fracture resistance of the membranes at a lower temperature, and the former was a more significant factor that weakens the fracture resistance of PEMs under the simulated operating conditions in fuel cells. These behaviors were explained in terms of cation and water interactions with the molecular structure of PFSA polymers.

Acknowledgements

The authors thank Dr. Dennis E. Curtin from DuPont® Corp. for providing Nafion® NRE211 membranes used in this study. We would also like to thank Dr. Juergen Keller from Fraunhofer IZM in Berlin for modifying the bulge testing device and Prof. William D. Nix from Stanford University for helpful discussions in the data analysis.

References

[1] S.J. Hamrock, M.A. Yandrasits, J. Macromol. Sci. C: Polym. Rev. 46 (2006) 219–244.
[2] K.A. Mauritz, R.B. Moore, Chem. Rev. 104 (2004) 4535–4585.
[3] S. Kundu, L.C. Simon, M. Fowler, S. Grot, Polymer 46 (2005) 11707–11715.
[4] H. Wang, G.A. Capuano, J. Electrochem. Soc. 145 (1998) 780–784.
[5] T. Okada, Y. Ayato, M. Yuasa, I. Sekine, J. Phys. Chem. B 103 (1999) 3315–3323.
[6] D.A. Dillard, Y. Li, J.R. Grohs, S.W. Case, M.W. Ellis, Y.-H. Lai, M.K. Budinski, C.S. Gittleman, J. Fuel Cell Sci. Technol. 6 (2009) 031014–031021.
[7] Y. Li, D.A. Dillard, S.W. Case, M.W. Ellis, Y.-H. Lai, C.S. Gittleman, D.P. Miller, J. Power Sources 194 (2009) 873–879.
[8] J.R. Grohs, Y. Li, D.A. Dillard, S.W. Case, M.W. Ellis, Y.-H. Lai, C.S. Gittleman, J. Power Sources 195 (2010) 527–531.
[9] Y. Kawano, Y. Wang, R.A. Palmer, S.R. Aubuchon, Polímeros 12 (2002) 96–101.
[10] C.M. Muscat-Fenech, A.G. Atkins, Int. J. Fract. 67 (1994) 69–80.
[11] Y. Li, J.K. Quincy, S.W. Case, M.W. Ellis, D.A. Dillard, Y.-H. Lai, M.K. Budinski, C.S. Gittleman, J. Power Sources 185 (2008) 374–380.
[12] Y. Tang, A.M. Karlsson, M.H. Santare, M. Gilbert, S. Cleghorn, W.B. Johnson, J. Mater. Sci. 425 (2006) 297–304.
[13] S. Cleghorn, J. Kolde, W. Liu, in: W. Vielstich, A. Lamm, H. Gasteiger (Eds.), Handbook of Fuel Cells, vol. 3, John Wiley and Sons Ltd, Chichester, England, 2003.
[14] T.D. Gierke, G.E. Munn, F.C. Wilson, J. Polym. Sci. B: Polym. Phys. 19 (1981) 1687–1704.
[15] W.Y. Hsu, T.D. Gierke, Macromolecules 15 (1982) 101–105.
[16] G. Gebel, Polymer 41 (2000) 5829–5838.
[17] A. Kusoglu, M.H. Santare, A.M. Karlsson, S. Cleghorn, W.B. Johnson, J. Polym. Sci. B: Polym. Phys. 46 (2008) 2404–2417.
[18] A.L. Yeager, A. Steck, J. Electrochem. Soc. 128 (1981) 1880–1884.
[19] J.R. Bontha, P.N. Pintauro, Chem. Eng. Sci. 49 (1994) 3835–3851.
[20] R. Tandon, P.N. Pintauro, J. Membr. Sci. 136 (1997) 207–219.
[21] T. Okada, H. Satou, M. Okuno, M. Yuasa, J. Phys. Chem. B 106 (2002) 1267–1273.
[22] S.H. de Almeida, Y. Kawano, J. Therm. Anal. Calorim. 58 (1999) 569–577.
[23] P.W. Majsztrik, A.B. Bocarsly, J.B. Benziger, Macromolecules 41 (2008) 9849–9862.
[24] Y. Tang, A. Kusoglu, A.M. Karlsson, M.H. Santare, S. Cleghorn, W.B. Johnson, J. Power Sources 175 (2008) 817–825.
[25] M.B. Satterfield, J.B. Benziger, J. Polym. Sci. B: Polym. Phys. 47 (2009) 11–24.
[26] A. Kusoglu, Y. Tang, M. Lugo, A.M. Karlsson, M.H. Santare, S. Cleghorn, W.B. Johnson, J. Power Sources 195 (2010) 483–492.
[27] F. Bauer, S. Denneler, M. Willert-Porada, J. Polym. Sci. B: Polym. Phys. 43 (2005) 786–795.
[28] J.T. Hinatsu, M. Mizuhata, H. Takenaka, J. Electrochem. Soc. 141 (1994) 1493–1498.
[29] A.Z. Weber, J. Newman, J. Electrochem. Soc. 151 (2004) 311–325.